Polariton physics/Physique des polaritons

Soliton physics with semiconductor exciton–polaritons in confined systems

Physique des solitons avec des polaritons excitoniques semiconducteurs dans des systèmes confinés

Maksym Sich [a], Dmitry V. Skryabin [b,c], Dmitry N. Krizhanovskii [a,*]

[a] *Department of Physics and Astronomy, The University of Sheffield, Sheffield, S3 7RH, United Kingdom*
[b] *Department of Physics, University of Bath, Bath, BA2 7AY, United Kingdom*
[c] *ITMO University, Kronverksky Avenue 49, Saint Petersburg, 197101, Russian Federation*

ARTICLE INFO

ABSTRACT

In the past decade, there has been a significant progress in the study of non-linear polariton phenomena in semiconductor microcavities. One of the key features of non-linear systems is the emergence of solitons. The complexity and the inherently strong nonlinearity of the polariton system made it a perfect sandpit for observing solitonic effects in half-light half-matter environment. This review focuses on the theory and the latest experimental elucidating physics as well as potential applications of conservative and dissipative solitons in exciton–polariton systems.

© 2016 Académie des sciences. Published by Elsevier Masson SAS. This is an open access article under the CC BY license (http://creativecommons.org/licenses/by/4.0/).

RÉSUMÉ

Au cours de la dernière décennie s'est opéré un progrès significatif dans l'étude des phénomènes non linéaires de polaritons dans des microcavités à semiconducteurs. Un des phénomènes caractéristiques des systèmes non linéaires est l'émergence de solitons. La complexité et la forte non-linéarité inhérente au système de polaritons en fait un parfait terrain de jeu pour observer des effets solitoniques dans un environnement mi-lumière mi-matière. Cet article passe en revue la théorie et les tout derniers développements physiques expérimentaux ainsi que des applications potentielles des solitons conservatifs et dissipatifs dans les systèmes de polaritons excitoniques.

© 2016 Académie des sciences. Published by Elsevier Masson SAS. This is an open access article under the CC BY license (http://creativecommons.org/licenses/by/4.0/).

* Corresponding author. Tel.: +44 (0)114 2224295; fax: +44 (0)114 2223555.
E-mail address: d.krizhanovskii@sheffield.ac.uk (D.N. Krizhanovskii).

1. Introduction

Solitons are non-spreading self-localised wavepackets. The first soliton has been described by John Scott Russell in 1834 [1], who observed an isolated non-spreading water wave moving across the Union canal near Edinburgh. With the development of high power pulsed lasers in 1970–1980's, it became possible to investigate optical solitons through the formation of non-diffracting beams and non-dispersing pulses of light propagating in bulk materials or optical fibres with a $\chi^{(3)}$ nonlinearity [2]. Picosecond pulse narrowing and splitting of the initial pulse into several peaks with increasing pulse power has been observed in 1980 in optical fibres with anomalous group velocity dispersion [3,4], which is essential for soliton formation in the case of positive (self-focusing) nonlinearity. Soliton phenomena in single-mode fibres and in many other systems can be described using nonlinear Schrödinger equations, which has become a paradigm model in soliton physics.

Matter wave solitons have been demonstrated in the clouds of Bose-condensed atoms placed in a magnetic trap. The interactions between atoms were tuned from repulsive to attractive via Feshbach resonance which cancels the dispersive spreading induced by the kinetic energy of atoms [5]. Multiple matter-wave solitons were observed bouncing in the trap and interacting amongst themselves repulsively [6]. It was also possible to observe bright solitons with condensates consisting of repulsively interacting atoms by altering the sign of the matter wave dispersion using optical lattice potentials [7]. Similarly, solitonic effects with light beams have been observed in nonlinear materials with periodic spatial modulation [8].

Self-localised structures existing in a dissipative system with an external supply of energy are often called *dissipative solitons* [9,10]. The balance between dispersion and nonlinearity for the dissipative solitons is also accompanied by the loss-gain balance. Dissipative solitons in optical resonators have been observed, e.g., in the vertical cavity surface emitting semiconductor lasers (VCSELs) operating in the bistable regime [11,12]. VCSEL solitons can be switched on/off using an external writing pulse, which makes them potentially suitable for applications in optical information processing.

Microcavity polaritons, which arise from strong exciton–photon coupling in semiconductor microcavities, attracted significant interest in the last decade [13–16]. The excitonic component in the polariton wavefunctions leads to strong repulsive polariton–polariton interactions and hence to a strong de-focusing nonlinearity. In fact, the interaction energy between two polaritons confined in 1-μm² area was measured in the range of 2–10 μeV [17], implying $\chi^{(3)}$ polariton nonlinearity to be two to three orders of magnitude higher than nonlinearity in VCSELs operating in the weak-coupling regime [18], bringing down the threshold powers required for observation of bistability, parametric wave mixing, and soliton formation. The two-dimensional nature of the polariton system allows one to address particular polariton states in energy–momentum space using external laser sources of relatively weak optical power, whereas the giant optical nonlinearity and fast ps response time of the polariton system are favourable to the development of polariton devices with applications in all-optical signal processing and switching [19,20].

Non-equilibrium polariton Bose condensates have been observed under non-resonant (above band gap) pumping [21,22], where it was suggested that polariton–polariton scattering plays an essential role in the convergence to the condensate state. One of the most remarkable properties of the interacting polaritons is the superfluid-like behaviour [23]. In the case when a polariton condensate flowing with a finite momentum interacts with a defect, suppression of polariton backscattering is observed, which is attributed to the renormalisation of the condensate excitation spectrum from parabolic to sonic-like due to polariton–polariton interactions at high particle density. While condensation is characterised by localisation of the polariton density in momentum space and formation of an extended state in real space, the soliton formation is associated with the localisation in real space and spectral broadening in momentum space.

In what follows, we will discuss the theory and experimental results on conservative and dissipative polariton solitons in planar polaritonic superfluids [24,25], in modulated polaritonic microcavity waveguides (microwires) [26], in slab waveguides [27] and in two-dimensional microcavity lattice potentials [28]. A particular emphasis will be paid to the role of the polariton polarisation (pseudo-spin) and formation of the so-called vector polariton solitons in both conservative [29] and dissipative [30] systems. Here, the spin-dependent anisotropy in the polariton–polariton interaction is important, and can lead to the vector solitons, whose polarisation oscillates rapidly in time and space.

2. Theory of exciton–polariton solitons in microcavities

2.1. Model equations

Non-propagating (zero momentum) modes in an ideal planar microcavity can be represented using the basis of circular polarizations $\sigma_\pm$, which couple with the ±1-spin excitons inside the quantum wells. Similarly, the propagating (non-zero momentum) modes occupied by moving bright solitons can be represented by a TE mode, where the non-zero electric field component is parallel to the mirrors and perpendicular to the momentum, and a quasi-TM mode, with a dominant electric field component aligned with the momentum and a small component perpendicular to the mirrors. The quasi-TM mode is directly associated with the small momentum-dependent energy splitting between the two modes, which becomes zero for the zero-momentum case.

The equations for the photonic modal amplitudes $E_{x,y}$ in the TE–TM representation are [30]:

$$\partial_t E_{x,y} - \mathrm{i}d(1 \pm \alpha)\nabla^2 E_{x,y} + (\gamma_\mathrm{p} - \mathrm{i}\delta_\mathrm{p})E_{x,y} = \mathrm{i}\,\Omega_\mathrm{R}\psi_{x,y} + (a \pm b)E_\mathrm{p}\,\mathrm{e}^{\mathrm{i}k_\mathrm{p}x} \tag{1}$$
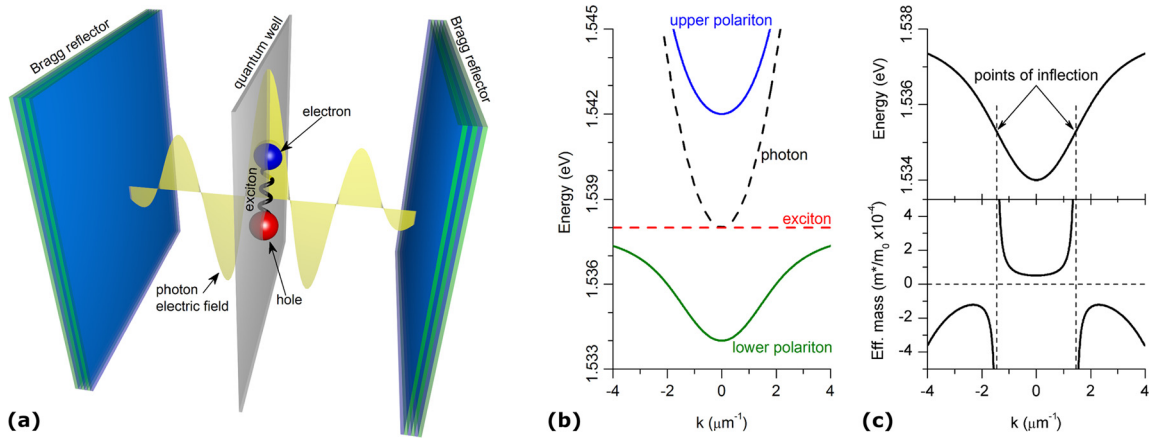
Fig. 1. (a) Schematic of a microcavity with quantum well positioned at an antinode of a photon mode. (b) Simulated polariton dispersion of a typical GaAs microcavity. Black dashed line is dispersion of uncoupled photons, red dashed – uncoupled exciton, blue solid – upper polariton branch, and green solid – lower polariton branch. (c) Lower polariton branch, upper panel, and corresponding effective mass, lower panel, as a ratio to free electron mass (m_0) show two points of inflection which divide regions of positive and negative effective masses of polaritons.

In the above equation, E_p and k_p are the pump amplitude and transverse momentum, while γ_p and δ_p are the photon decay rate and detuning, Ω_R is the Rabi frequency and d is the photon dispersion coefficient. Relative values of a and b ($|a|^2 + |b|^2 = 1$) control the pump polarisation. The momentum dependence of the TM and TE polariton eigenfrequencies can, in general, be characterized by serial expansions of both kinetic energy and the Rabi frequency in even (for the ideal planar resonators) powers of the Laplacian. Here we are restricting ourselves to the leading-order approximation, with the α coefficient characterizing the splitting of the resonances. The amplitudes for the TE photonic and excitonic modes are linked with the ones for $\sigma_\pm$ polarizations as $E_y = i(E_+ - E_-)$, $\psi_y = i(\psi_+ - \psi_-)$. A similar transformation for the TM modes will, however, be only approximately valid since the component of the TM-mode perpendicular to the mirrors does not couple with excitons. This difference is, however, disregarded in our calculations, so that $E_x \simeq E_+ + E_-$, $\psi_x \simeq \psi_+ + \psi_-$. Note that we have chosen the pump momentum along the x-direction.

The equations for the $\sigma_\pm$ amplitudes of the excitonic field are

$$\partial_t \psi_\pm + \left(\gamma_e - i\delta_e + i|\psi_\pm|^2 - iV|\psi_\mp|^2 \right) \psi_\pm = i\,\Omega_R E_\pm \qquad (2)$$

Here $V \simeq 0.05$ is the relative strength of the inter-spin attraction, γ_e is the coherence decay rate and δ_e is the detuning of the excitonic resonance from the frequency of the pump field. Despite the fact that our approach ignores some details, such as coupling of the coherent excitons with the incoherent reservoir [31], inhomogeneities of the cavities and quantum wells and the exact account for the energy–momentum dependence at large momenta, it reproduces the main experimental observations related to polariton solitons and provides a solid theoretical framework for understanding solitonic effects in microresonators.

2.2. Families of conservative solitons

We start from the case when there is no pump ($E_p = 0$), all the loss mechanisms are neglected (conservative limit) and polaritons have one polarization (e.g., σ_+). Then, for the envelope function A of a polaritonic wavepacket with momentum $k = k_0$ and energy $\epsilon_0 = \epsilon(k_0)$ measured from the bottom of the lower polariton branch, one can derive the following 1D Gross–Pitaevskii (GP) equation [32]:

$$i\hbar\partial_t A = -i\epsilon'\partial_x A - \frac{1}{2}\epsilon''\partial_x^2 A + g|A|^2 A, \quad \epsilon' = \partial_k \epsilon(k_0), \quad \epsilon'' = \partial_k^2 \epsilon(k_0) \qquad (3)$$

Here $\epsilon'/\hbar = v$ is the group velocity, while $\hbar^2/\epsilon'' = m_x^*$ is the effective polariton mass (see Fig. 1). ϵ'' of the lower branch polaritons becomes zero at some critical momentum corresponding to the so-called magic angle. $g > 0$ is the effective nonlinearity, which is also momentum dependent [32]. Note that when we add the second dimension y, we will find that the effective mass in the y-direction (perpendicular to the direction of polariton flow) m_y^*, always stays positive.

A family of dark soliton solutions, existing for the $m_x^* > 0$ is given by

$$A = \sqrt{\frac{q}{g}} \left(\tanh(\tau\sqrt{q}\cos\phi)\cos\phi - i\sqrt{q}\sin\phi \right) e^{-iqt/\hbar} \qquad (4)$$

where $\tau = \sqrt{\frac{2}{\epsilon''}}(x - t\epsilon'/\hbar) - \frac{1}{\hbar}t\sqrt{q}\sin\phi$. These are the solutions which have been observed in the experiments with the polaritonic flow scattered by a cylindrical obstacle [33,24]. ϕ is the greyness parameter ($\phi = 0$ corresponds to the black

solitons), which also determines the soliton velocity shift with respect to the group velocity of the linear polaritons. $q > 0$ is the parameter determining polariton density in the soliton background, $N = q/g$. The soliton core width is given by the so-called 'healing length': $l = \hbar/\sqrt{2m^*Ng}$.

If the nonlinear interaction between the $\sigma_\pm$ polariton branches is accounted for, then Eq. (3) is replaced by coupled GP equations. The relatively weak cross-spin interaction favours the existence of so-called half-solitons, when the polariton density in one component is quasi-constant across the soliton core in the other component [34,29]. Conservative solitons in a system with losses exist only as adiabatically decaying quasi-solitons. To claim the soliton observation, the decay time ideally should be longer than the characteristic time of the dispersive spreading, which in the energy units implies that the polariton linewidth is less than two nonlinear energy shift, $\gamma_p\hbar < 2gN$. Using the polariton basis, as opposed to the equations for the photonic and excitonic fields, also has its limitations. In particular, it has been formally shown in Ref. [35] that a new class of the dark soliton solutions and vortices can exist in the full model in the regime of the so-called 'intrinsic bistability', which is possible providing the cavity and excitonic resonances do not coincide. For these new solutions, the soliton core in the excitonic component can become arbitrarily narrow, while the one for the photonic component stays wide, so that the excitonic part of the dark soliton is only weakly influenced by the photonic one [36].

The stability of the conservative dark solitons in the polaritonic condensates has not been studied in detail yet, but preliminary results [35] indicate that using the two-component photon–exciton model introduces a drift instability absent in the GP approach. This, in part, can be related to the fact that the GP approach can not capture all the dynamical features if the excitonic and cavity resonances do not coincide. Families of conservative solitons and their stability in the two-spin model have not been studied yet. In this regard, one can expect differences with respect to nonlinear optics, where the self- and cross-spin interactions have the same sign. Also, more formal mathematical studies of the half-soliton regime can be beneficial both to the interpretation of the existing studies and to guidance of the forthcoming experiments. We should also mention here that accounting for the second transverse dimension is well known to lead to the break-up of the dark soliton stripes into trains of vortices with alternating polarities [37].

A family of bright solitons existing for the $m_x^* < 0$ is given by

$$A = \sqrt{\frac{2q}{g}}\operatorname{sech}\left(\sqrt{\frac{2q}{|\epsilon''|}}(x - \frac{1}{\hbar}|\epsilon''|vt)\right)e^{-i\frac{1}{\hbar}qt - ivx + i\frac{1}{2\hbar}|\epsilon''|v^2t} \tag{5}$$

The above solitons are probably the most obvious candidates, not only for experimental observations, but also for practical applications. However, they are still the least studied of all possible polariton–solitons.

The GP equation (3), becomes invalidated, when the essential part of the soliton spectrum overlaps with the point where the effective mass changes its sign, so that the soliton existence conditions become violated. This is the case for both bright and dark solitons. The GP model can be generalised by including the higher-order terms in the serial expansion of $\epsilon(k)$. In particular, the third-order derivative term becomes the leading order term around the point $m_x^* = \infty$. This observation brings a connection with the significant volume of knowledge generated in the fibre optics community about the role this term plays in soliton dynamics and, in particular, in frequency conversion and supercontinuum generation [4]. Regarding the latter, the so-called Cherenkov radiation emission by solitons and mixing of solitons with dispersive radiation [4], which are different from the familiar parametric processes relying on the phase-matching of dispersive waves only, still have not been studied in the polaritonic context.

2.3. Dissipative polariton solitons

If a resonant pump is applied ($E_p \neq 0$), then the losses are compensated and non-decaying cavity solitons can exist [32,38–40]. Theory of polariton–solitons in microresonators has many common features with the theory developed for non-polariton cavity solitons [10,41,42], but it has important novel aspects as well. An obvious one is that the effective mass changes its sign as momentum varies, so it can have different values and signs in the two transverse directions. In the polariton basis, the GP model can be generalised to include losses (γ), pump (P) and higher order dispersions (ϵ'''). The resulting equation is usually referred to as the generalised Lugiato–Lefever (gLL) model:

$$i\hbar\partial_t A = (\delta - i\gamma)A - i\epsilon'\partial_x A - \frac{1}{2}\epsilon''\partial_x^2 A + i\frac{1}{3!}\epsilon'''\partial_x^3 + g|A|^2 A - P, \quad \epsilon''' = \partial_k^3\epsilon(k_0) \tag{6}$$

Here δ is the energy offset between the lower branch polariton at k_0 and the pump photon. Diffraction along the second dimension has been disregarded, which can be useful to simplify numerical procedures and is physically justified if lateral confinement has been implemented (see, e.g., [32,43]). For $\gamma = \epsilon''' = 0$ and $\epsilon'' < 0$, the above equation has an analytical bright soliton solution [41]. For $P = 0$, this solution transforms into Eq. (5), while for $P \neq 0$ it splits into two branches, one (upper) stable and one (lower) unstable [41,42]. For $\epsilon''' \neq 0$, the soliton gets an oscillatory tail, while its velocity acquires a shift relative to $\epsilon'/\hbar$ [32].

Bright solitons in the full photon–exciton model have been studied in Refs. [32,25,30]. Polarization properties of these solitons appear to be highly relevant for their experimental observation [30]. In particular, if the pump field is either circularly (b or $a = 0$) or linearly ($|a| = |b|$) polarised, then the circularly polarised solitons are stable [30]. The linearly polarised
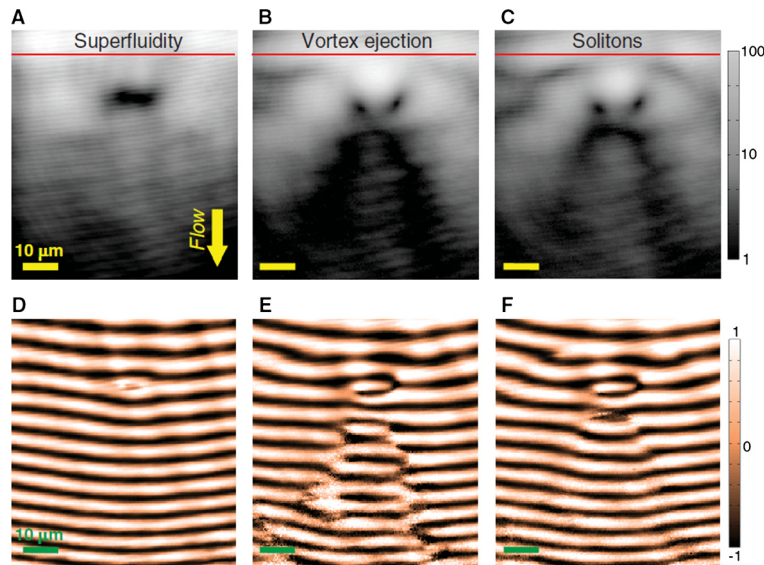
Fig. 2. (A to C) Real-space images of the polariton gas flowing downward at different excitation densities in the presence of a double defect (total width: 15 mm). The gas is injected above the red line. At high density (A) (117 mW), the fluid is subsonic ($v_{flow} = 0.25c_s$) and flows in a superfluid fashion around the defect. At lower densities (B) (36 mW; $v_{flow} = 0.4c_s$), a turbulent pattern appears in the wake of the defect, eventually giving rise to the formation of two oblique dark solitons (C) (27 mW; $v_{flow} = 0.6c_s$). (D to F) Interferograms corresponding to (A) and (C), respectively. From [24]. Reprinted with permission from AAAS.

solitons existing for the linearly polarised pump field can be considered as consisting of the two circularly polarised components, which interact repulsively ($V < 0$, $m_x^* > 0$), resulting in the exponential instability of these soliton states and their evolution towards the quasi-circularly polarised ones [30]. Thus $\sigma_\pm$-solitons are the preferential states for either choice of the pump polarization. These solitons can be subject to the oscillatory Hopf instability, as many other types of cavity solitons [42], providing losses are sufficiently small and pump is sufficiently strong.

The soliton existence based on the negative effective mass balanced by the defocussing nonlinearity apply only in the direction of the pump momentum. The reasons for the solitonic effects in the perpendicular direction are different; since the effective polariton m_y^* is positive, the parametric processes do not involve mixing of momenta with the non-zero y-projection. Hence if one takes an idealised model with $\partial_x = 0$, then the upper state of the polariton bistability loop is stable and so are the fronts connecting upper and lower branches of the polariton bistability loop [38–40]. These fronts taken at the pump frequency generally move along y, but the motion can be prevented by a pinning mechanism due to the presence of the localised polariton field components at the signal and idler energies. Thus a family of one-dimensional parametric solitons is formed. Families of 1D solitons in x and y coexist across a broad parameter range [38–40]. However, the 2D solitons, for which two different trapping mechanisms balance the diffraction out simultaneously, appear only in a very narrow range of the parameter space [38,39]. When the pump momentum is either zero or small, so that $m_{x,y}^* > 0$, then families of dissipative 1D and 2D dark solitons have been found and their dynamics were studied in detail in Refs. [44,45].

3. Experimental reports of polariton solitons

3.1. Conservative dark solitons in polariton superfluids

In [24] Amo et al. present their study of propagating polariton fluids in microcavities resonantly excited with an external laser beam at a finite k-vector. Solitons and vortices develop in the unpumped region where polaritons propagate out of the excitation spot. In this respect, the polariton system can be treated by the Gross–Pitaevskii equation with losses but without gain [33], as mentioned in the previous section.

The main experimental result is presented in Fig. 2. At subsonic speeds (the speed of polariton v_{flow} is about 1/4 of the speed of sound, c_s, of polariton condensate excitations), the polariton condensate is in superfluid regime. When it hits a large defect (dark region), polariton scattering is suppressed, as evidenced by the absence of density modulation. We note that such a suppression of scattering can not be attributed simply to the screening of the potential barrier, since there is still a zero polariton density observed in the region of the defect. As the excitation density and hence the speed of sound are decreased, low-density channels are observed in the wake created by the defect. The interference pattern of the condensate emission and the plane wave reference beam reveals fork-like dislocations along these low-density channels, which are related to the passage of vortices with orbital angular momentum $M = \pm 1$. The system enters a so-called turbulent regime. Finally, at even lower densities, the fork-like dislocations in the interference pattern transform into phase jumps of π, characteristic of oblique dark solitons. Similar results were also obtained by Grosso et al. with the pulsed excitation [46].
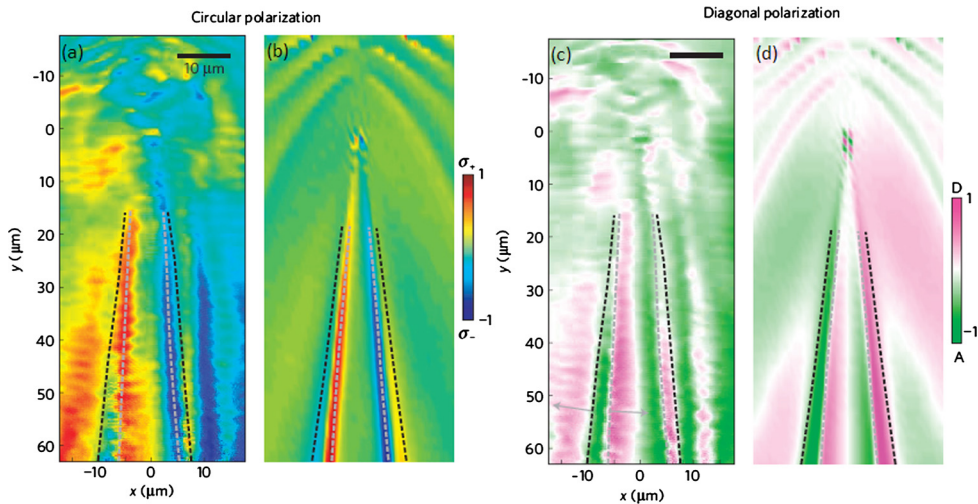
Fig. 3. (a), (c) The measured degree of circular and diagonal polarisations, respectively; (b), (d) The calculated patterns from the solution to the nonlinear spin-dependent Schrödinger equation. The dashed lines show the trajectory of the inner (grey) and outer (black) half-solitons. The trajectories of the half-solitons appear as extremes of circular polarization, and as domain walls in diagonal polarization. The grey arrows in (b) indicate the direction of acceleration of the half-solitons induced by the effective magnetic field.

Adapted by permission from Macmillan Publishers Ltd: Nature Physics [29], copyright 2012.

Note that Ref. [47] has questioned whether the experimental results in [24] can be considered as the definitive observations of the dark polariton solitons or can be partly interpreted as the linear interference effects. Nevertheless, side-by-side comparison of linear and non-linear regimes strongly supports the dark soliton interpretation [48].

Furthermore, the break-up of dark solitons into pairs of circularly cross-polarised dark half-solitons has been predicted [34] and observed [29], as shown in Fig. 3. This effect occurs because of the presence of an effective in-plane magnetic field [49], arising from the polarisation splitting between the transverse electric (TE) and transverse magnetic (TM) cavity modes. The effective magnetic field, which interacts with polariton pseudospin (polarisation) in similar way as the Coulomb force does with charges, splits the integer soliton into a pair of oblique half-solitons with opposite polarisations. In this respect, such mixed pseudospin-phase excitations behave like one-dimensional topological magnetic monopoles. In microcavities resonantly pumped with a laser at normal incidence, oblique spinor half-solitons were also predicted to emerge out of a Skyrmion lattice in the non-linear optical spin Hall regime due to the presence of TE–TM splitting and spin-dependent polariton–polariton interactions [50].

3.2. Polariton gap solitons in periodic lattices

The periodic spatial modulation of a medium creates an artificial band structure with energy gaps and normal polariton dispersion described by negative effective mass. In the presence of nonlinearity given by effective repulsive interactions between polaritons, spatially self-localized states may appear within the energy gaps. These states, known as bright gap solitons (GSs), are metastable solutions to the Gross–Pitaevskii equation [51]. In contrast to continuous systems, discrete solitons in array lattices represent collective excitations of the nonlinear chain as a whole.

Tanese et al. [26] have demonstrated the formation of gap solitons in 1D semiconductor microcavity wires with a modulated thickness under both continuous wave and pulsed nonresonant excitation. The periodically modulated width (the modulation period is $P = 2.7$ μm and the wire width is modulated between $W_{min} = 1.9$ μm and $W_{max} = 2.8$ μm) of the wires results in a periodic modulation of the cavity mode energy, which in turn creates a periodic potential for the polariton states. Such a periodic potential leads to the formation of polariton mini-Brillouin zones (MBZ) separated by energy gaps in energy–momentum space. The size of the MBZ is given by the modulation period: $k_{MBZ} = \pi/P$, and the energy gap is determined by the amplitude of the modulation.

Above a certain threshold, polaritons can spontaneously condense into localised states with energy in the band gap. Depending on the excitation power, either condensation into an anti-symmetric bright gap soliton state (S1, Figs. 4(a, c)) or a symmetric localised defect state (S2, Figs. 4(b, d)) occurs. The wavefunction of the S1 state extends over many periods of the realspace lattice, while in momentum space, it has maxima at the edges of MBZ where polariton effective mass $m^* < 0$, which is characteristic of the gap soliton. Analytically the spatial profile of the bright gap soliton is described by sech^2 function [26], in agreement with in the experimental results. By contrast, at higher pump power, the substantial energy blueshift of the condensed polaritons into the gap leads to a defect state S2, which is strongly localised in realspace with an exponentially decaying amplitude profile. A linear combination of the S1 and S2 states can be also observed at intermediate powers.
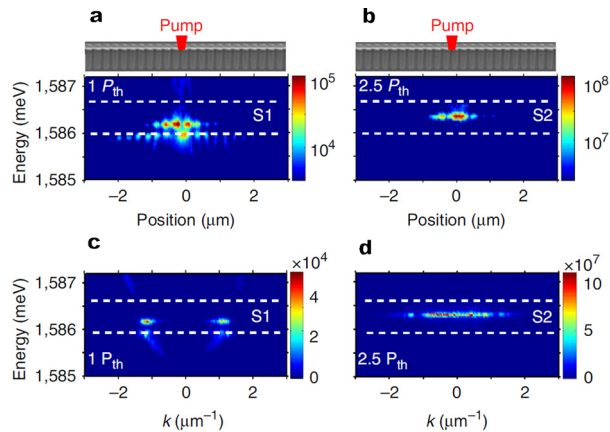
Fig. 4. A modulated wire is excited with a 2 μm CW laser spot centred on a maximum of the periodic potential (narrow region of the wire). Total emission intensity measured from a single modulated wire as a function of the excitation power. (a, b) Spectrally and spatially resolved emission for two excitation powers (in logarithmic colour scale). (c, d) Spectrally resolved far-field emission measured on the same wire for the same excitation powers (in linear colour scale); the first mini-gap induced by the periodicity is indicated with dashed lines.
Adapted by permission from Macmillan Publishers Ltd: Nature Communications [26], copyright 2013.
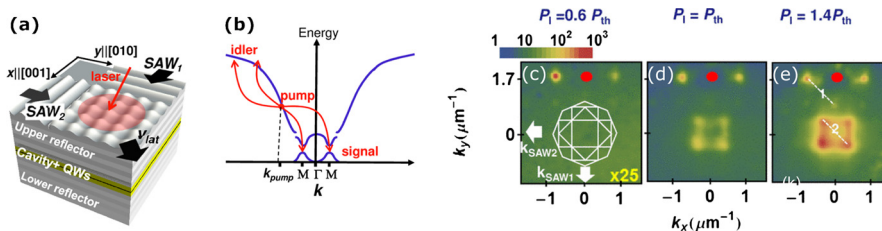

Fig. 5. (a) Square lattice for polaritons created by the interference of two surface acoustic waves (SAWs) propagating along the $\hat{x} = [010]$ and $\hat{y} = [001]$ surface directions of a (100)–(Al, Ga) As microcavity. The lattice moves along the $(\hat{x} + \hat{y}) = [110]$ direction with a velocity of $\upsilon_{lat} = \sqrt{2}\upsilon_{SAW}$, where $\upsilon_{SAW} = 3$ μm/ns is the SAW phase velocity. (b) Schematic representation of the OPO process in the modulated polariton dispersion along $\Gamma \to M$. The pump state is generated by tuning the laser energy and angle of incidence. Above the threshold of formation of the PMCP polaritons scatter into the signal and idler states, as indicated by the arrows. (c) k-space PL image of an incoherent polariton gas. The red point at $\mathbf{k}_p = (k_{p_x}, k_{p_y}) = (0, 1.7)$ μm^{-1} marks the blocked pump state. The PL peaks on the sides are the diffracted pump beams. The white lines delineate the first four MBZs. (d, c) are the corresponding images at $P_l = P_{th}$ and $P_l = 1.4P_{th}$.
Adapted from [28].

Cerda-Méndez et al. [28] have further shown the formation of polariton gap soliton states in 2D dynamic microcavity lattices created by perpendicular surface acoustic waves (SAW) with wavelength $\lambda_{SAW} \approx 8$ μm (Fig. 5(a)) in the optical parametric oscillator (OPO) regime (Fig. 5(b)). In this case, the periodic potential is mainly created due to spatial modulation of the exciton level, whereas the square lattice results in mini-Brillouin zones (MBZs) of dimension $k_{SAW} = 2\pi/\lambda_{SAW}$ separated by the energy gaps. In a homogeneous microcavity, polariton macroscopic coherent phases (PMCPs) originating from stimulated polariton–polariton scattering from the pump normally appear at the lowest energy state with zero in-plane momentum. By contrast, in the presence of SAW of moderate amplitude, PMCPs are excited via the accumulation of particles at critical points of negative mass with energies above the ground state level (Figs. 5(c–e)), which is indicative of the formation of a bright gap soliton.

3.3. Conservative bright polariton solitons in semiconductor waveguides

In Ref. [27], Walker et al. used planar AlGaAs/GaAs waveguides with InGaAs quantum wells embedded in the core, where a propagating waveguide photonic mode formed by total internal reflection strongly couples to quantum well excitons, see Fig. 6(a). Compared to microcavities, the waveguide system has the advantages of an order of magnitude faster polariton velocity (30–50 μm/ps, Fig. 6(b)), simplicity of the design, and fabrication and compatibility with existing designs of high-performance waveguide photonic circuit elements.

The effective mass on the lower polariton branch is negative at any momentum (Fig. 6(b)), so formation of bright solitons is expected, since polariton–polariton interactions are repulsive. In Ref. [27] a sub-picosecond pulse with energy resonant with the lower polariton branch is injected into the waveguide via grating coupler (Fig. 6(a)). The output pulse duration and its spectrum are detected after the pulse propagates 600 μm. At low excitation power the initial pulse broadens from 350 fs to 4 ps due to large polariton group velocity dispersion. By contrast, as the pulse power is increased to about 0.5 pJ, the duration of the output pulse narrows below the resolution 2 ps (Fig. 6(c)). Such temporal compression is indicative
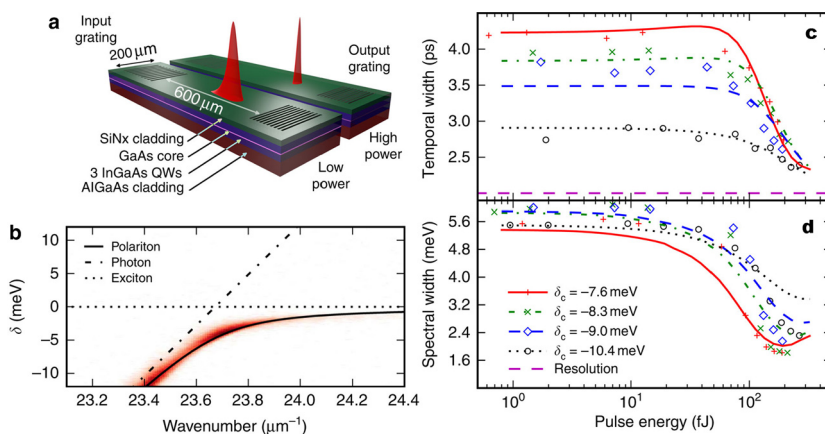
Fig. 6. (a) Schematic diagram of waveguide (the same waveguide is shown with pulses under low-power and high-power excitation conditions). (b) Angle-resolved photoluminescence spectrum showing emission from the lower polariton branch in red. The fitted polariton dispersion (solid line) is shown with the uncoupled exciton and photon modes, which would exist for zero light matter coupling (dotted and dashed lines). The horizontal and vertical axes are respectively the wavenumber of the guided mode and the detuning δ between polariton and exciton energies. (c) Experimental (symbols) and numerically simulated (line) pulse temporal duration versus pulse energy inside the waveguide for a number of detunings δ_c of the central pulse frequency from the exciton. (d) Experimental (symbols) and numerically simulated (lines) pulse spectral width versus pulse energy for the same detunings. Adapted from [27].
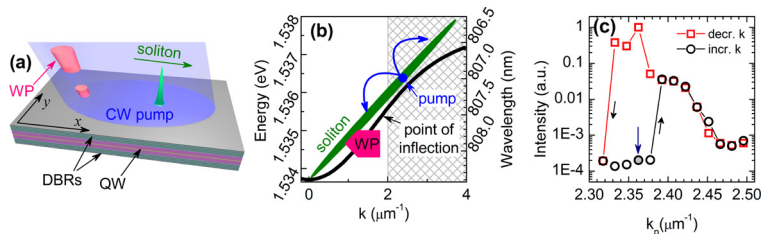

Fig. 7. (a) Schematic diagram of experiment. A large area of the sample is quasi-resonantly illuminated with a continuous wave (CW) pump. A picosecond writing pulse (WP) (red) triggers the soliton pattern formation. (b) Polariton dispersion (solid black curve) of the lower polariton branch (LPB). The schematic location of the pump and WP in energy–momentum space are shown; in the experiment the shaded area above $k > 2~\mu\text{m}^{-1}$ is blocked in the detection path to avoid saturation of the detectors by the reflected pump and WP beams. (c) Bistable polariton density as a function of pump momentum. Arrow indicates the state of the system created by the pump before incidence of the writing pulse. Adapted from [25].

of the bright soliton. Further proof of the bright soliton is revealed by measuring the time of flight of different frequency components. In the soliton regime, the frequency dependence of the time of flight is cancelled since all harmonics travel at the same speed. From the soliton formation threshold, a nonlinear refractive index three to four orders of magnitude larger than in any other ultrafast optical systems (based on silicon, InGaP or AlGaAs in the weak coupling regime) was deduced, which verifies the highly nonlinear nature of the polariton platform.

3.4. Propagating bright dissipative polariton solitons

While above we mainly focused on the conservative soliton system, where the role of the pump can be neglected, in this section the results on the observation of propagating dissipative polariton solitons are summarised. Here, the pump plays an important role. Namely, a dissipative soliton is excited when the pump is tuned slightly above the polariton resonance at k-vectors, where polaritons have a negative effective mass. In this case, the pump field inside the microcavity exhibits bistable behaviour as a function of pump power. The dissipative soliton can be considered as a local switch from the lower to the upper state of the bistabile pump field. Moreover, broadband polariton–polariton scattering results in population of the broad spectrum in momentum space, fully compensating polariton losses and leading to a stable localised state: a dissipative soliton.

In 2012, Sich et al. [25] presented the first experimental observation of such a bright 2D dissipative polariton soliton propagating in a semiconductor GaAs microcavity with InGaAs quantum wells. The scheme of the experiment is shown in Figs. 7(a, b). A continuous wave (CW) *pump* laser is applied at a k-vector k_p, which is above the point of inflection of the lower polariton branch (LPB). The pump beam is focused to a 70 μm (full width at half-maximum, FWHM) Gaussian spot. The lower polariton branch is driven quasi-resonantly by the pump laser, so that the internal polariton field exhibits bistable behaviour as a function of the pump k-vector (k_p), as shown in Fig. 7(c). A writing pulse (WP) with a duration of 5 ps triggers soliton formation.
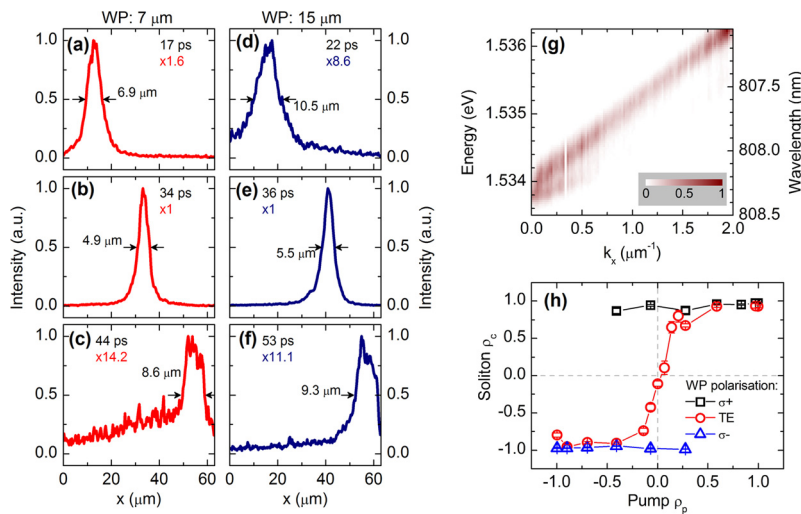
Fig. 8. (a–c) Experimentally measured spatial intensity profiles of a soliton created by the 7-μm writing pulse at different times, showing excitation and decay of the soliton. (d–f) Intensity profiles of a soliton created by the 14-μm writing pulse. (g) Intensity distribution of emission from a single soliton in E–k_x space taken at $k_y = 0$ within $\Delta k_y = 0.1$ μm^{-1}. (h) Soliton CPD, ρ_c, as a function of pump CPD, ρ_p, recorded for the case of σ_+, σ_- circularly polarised and TE linearly polarised WB (circles, squares and triangles, respectively). Adapted from [25,30,52].

The effect of self-focusing of the polariton wavepacket excited by WP, which is characteristic of soliton formation, is shown in Fig. 8. The soliton size, as mentioned before, is determined by a combination of the cavity and pump parameters, and is expected to be of the order of 2 μm [32] – smaller than the experimental resolution of ≈5 μm. At first, a 7-μm WP is used (Figs. 8(a–c)), then a 14-μm WP is applied (Figs. 8(d–f)). In both cases, the soliton size along the direction of propagation (x axis) is measured to be ≈ 5 μm, which confirms the prediction above. Furthermore, the measured dispersion of the soliton in Fig. 8(g) shows a linear dependence in the broad range of k-vectors down to $k = 0$, as is expected for a non-dispersive solitonic wavepacket. Notably, the dissipative soliton propagating with the same velocity can be excited using WPs of different k-vectors and energies: self-organised polariton–polariton scattering from the pump, and not the WP, defines the soliton properties. We note that localisation in the y-direction is also observed due to the presence of the localised polariton field components at the signal and idler energies, as predicted theoretically. Therefore, a 2D spatial microcavity polariton soliton is formed.

In reference [30], Sich and co-authors investigated the effect of spin-dependent polariton–polariton interactions on the formation of circularly and linearly polarised solitons. It was found that when the background CW pump and the WP which triggers the soliton are circularly co-polarised, then solitons with the same circular polarisation are excited. Once triggered, the soliton maintains its polarisation during propagation over macroscopic distances, indicating phase synchronisation between the nondegenerate TE and TM polarised polariton modes. If the pump is linearly polarised, then solitons with either σ_+ or σ_- circular polarisation can be triggered by a WP with the corresponding circular polarisation due to the very different interaction strengths between circularly co- and cross-polarised polaritons (circularly co-polarised polaritons strongly repel, whereas circularly cross-polarised polaritons weakly attract). Fig. 8(h) shows a systematic study of the soliton circular polarisation degree (CPD), ρ_c, as a function of the pump CPD, ρ_p, for the cases of σ_+, σ_- and linearly polarised WPs, where CPD is defined as $\rho = (|E_+|^2 - |E_-|^2)/(|E_+|^2 + |E_-|^2)$. It shows that σ_+ (σ_-) polarised spatially localised pulses can be excited in the range of ρ_p from 1 to -0.25 (-1 to 0.25) using σ_+ (σ_-) polarised WPs. Thus solitons can be excited under a linearly or circularly polarised pump at the same pump power. There is a range ρ_p from about -0.25 to 0.25 when both σ_+ and σ_- polarised solitons can be triggered. For the linearly polarised WP, the slight bias of ρ_p towards σ_+ or σ_- polarisations by 0.1 quickly ensures excitation of either σ_+ or σ_- circularly polarised solitons with $|\rho| \approx 0.85$–0.95, implying the stability of circularly polarised solitons if the symmetry is slightly disturbed.

Theoretically it was also found that linearly polarised solitons excited by a linearly polarised WP are unstable: it is more energetically favourable for the system to evolve into spatially separated cross-circularly polarised solitons, which keeps the energy of excited polaritons in resonance with the feeding pump. As a result, when both pump and WP are linearly polarised, a vector soliton is formed with circular polarisation rapidly oscillating in space/time.

In subsequent work, Chana et al. [52] have demonstrated formation of patterns of dissipative solitons by using WP pulse elongated along the propagation x direction or along the perpendicular y direction. Since the WP had a size of about 30 μm, much bigger than the size of a single soliton (5 μm) given by the interactions and cavity parameters, the polariton wavepacket injected by the WP is expected to break into multiple localised solitons. A similar effect is observed in the cold atom system, when an initially extended condensate cloud trapped in a parabolic potential breaks into repelling localised solitons with the change of atom interactions from repulsive to attractive via Feshbach resonance [6]. It was also predicted theoretically that each of these localised polariton solitons may have a multi-hump structure with several field
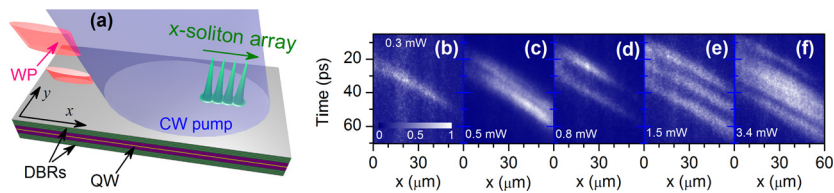
Fig. 9. (a) Experimental setup is similar to that shown in Fig. 7(a), but with a significantly elongated WP beam. (b–f) Emission intensities of a single soliton (b) and *x*-soliton arrays (c–f) for different WP powers recorded versus time and position *x*; $t \approx 0$ is the WP arrival time within an error of 5 ps. The pump beam is centred around $x = 30$ μm.
Adapted from [52].

maxima (from 2 to 5) across its profile separated by ≈ 2 μm. Multiple localised solitons following one another in space and time are observed in Fig. 9 for WP elongated along *x*. The size of an individual soliton in the *x*-array varies in the range from 7 to 14 μm, depending on the WP power, which is bigger than the soliton size observed for smaller WP. Such an observation suggests that individual solitons in the array may have a multi-hump structure, which is not spatially resolved in the experiment. Soliton separations in time of ≈ 10 ps in the *x*-arrays are potentially promising for the development of polaritonic devices operating at ≈ 100 Gbit/s, where solitons are used as data bits in logic gates [53]. By elongating the WP in the transverse *y* direction, it was also possible to observe stable *y*-soliton arrays formed perpendicular to the propagation direction, arising from changes of the front velocity across the propagating beam profile.

4. Conclusions and outlook

To conclude, we have summarised the theoretical and the experimental studies of families of polariton solitons in microcavities, wires, and waveguides. It is important to note that giant optical nonlinearity enables the formation of mesoscopic polariton solitons with the number of quasiparticles in the range of 100–1000. Squeezing of soliton states associated with increased/reduced fluctuations in the amplitude or phase of soliton emission above/below the quantum limit [54,55] may be an interesting direction to investigate. Additionally, spin-dependent polariton–polariton interactions may also lead to peculiar effects of polarisation squeezing in the soliton regime. On the other hand, there are proposals for the realisation of topological polariton insulators in microcavity structures [56] and waveguides [57] in the strong coupling regime. The strong nonlinearity may also enable the formation of topological solitons, the motion of which is entirely dictated by the topology of the engineered structures [58].

Acknowledgements

References

[1] J.S. Russell, Report on waves, in: Report of the British Association for the Advancement of Science, vol. 14, 1845, pp. 311–390, London, plus plates XLVII–LVII.
[2] L.F. Mollenauer, R.H. Stolen, J.P. Gordon, Experimental observation of picosecond pulse narrowing and solitons in optical fibers, Phys. Rev. Lett. 45 (13) (1980) 1095–1098, http://dx.doi.org/10.1103/PhysRevLett.45.1095.
[3] Y.S. Kivshar, G.P. Agrawal, Optical Solitons: From Fibers to Photonic Crystals, Academic Press, 2003.
[4] D.V. Skryabin, A.V. Gorbach, Colloquium: looking at a soliton through the prism of optical supercontinuum, Rev. Mod. Phys. 82 (2) (2010) 1287–1299, http://dx.doi.org/10.1103/RevModPhys.82.1287.
[5] L. Khaykovich, F. Schreck, G. Ferrari, T. Bourdel, J. Cubizolles, L.D. Carr, Y. Castin, C. Salomon, Formation of a matter-wave bright soliton, Science 296 (5571) (2002) 1290–1293, http://dx.doi.org/10.1126/science.1071021.
[6] K.E. Strecker, G.B. Partridge, A.G. Truscott, R.G. Hulet, Formation and propagation of matter-wave soliton trains, Nature 417 (2002) 150–153, http://dx.doi.org/10.1038/nature747.
[7] B. Eiermann, T. Anker, M. Albiez, M. Taglieber, P. Treutlein, K.-P. Marzlin, M.K. Oberthaler, Bright Bose–Einstein gap solitons of atoms with repulsive interaction, Phys. Rev. Lett. 92 (23) (2004) 230401, http://dx.doi.org/10.1103/PhysRevLett.92.230401.
[8] J.W. Fleischer, M. Segev, N.K. Efremidis, D.N. Christodoulides, Observation of two-dimensional discrete solitons in optically induced nonlinear photonic lattices, Nature 422 (2003) 147–150, http://dx.doi.org/10.1038/nature01452.
[9] N. Akhmediev, A. Ankiewicz-Kik (Eds.), Dissipative Solitons, Springer, 2005.
[10] T. Ackemann, W.J. Firth, G.-L. Oppo, Fundamentals and applications of spatial dissipative solitons in photonic devices, Chapter 6, in: P.R.B.E. Arimondo, C.C. Lin (Eds.), Advances in Atomic, Molecular and Optical Physics, in: Advances in Atomic, Molecular and Optical Physics, vol. 57, Academic Press, 2009, pp. 323–421.
[11] S. Barland, J.R. Tredicce, M. Brambilla, L.A. Lugiato, S. Balle, M. Giudici, T. Maggipinto, L. Spinelli, G. Tissoni, T. Knudl, M. Miller, R. Jager, Cavity solitons as pixels in semiconductor microcavities, Nature 419 (2002) 699–702, http://dx.doi.org/10.1038/nature01049.
[12] F. Pedaci, S. Barland, E. Caboche, P. Genevet, M. Giudici, J.R. Tredicce, T. Ackemann, A.J. Scroggie, W.J. Firth, G.-L. Oppo, G. Tissoni, R. Jager, All-optical delay line using semiconductor cavity solitons, Appl. Phys. Lett. 92 (1) (2008) 011101, http://dx.doi.org/10.1063/1.2828458.
[13] A. Kavokin, J.J. Baumberg, G. Malpuech, F.P. Laussy, Microcavities, Semiconductor Science and Technology, Oxford University Press, 2007.

[14] D. Sanvitto, V.B. Timofeev, Exciton Polaritons in Microcavities: New Frontiers, Solid State Sciences, vol. 172, Springer, 2012.

[15] H.M. Gibbs, G. Khitrova, S.W. Koch, Exciton–polariton light-semiconductor coupling effects, Nat. Photonics 5 (273) (2011) 275–282, http://dx.doi.org/10.1038/nphoton.2011.15.

[16] I. Carusotto, C. Ciuti, Quantum fluids of light, Rev. Mod. Phys. 85 (2013) 299–366, http://dx.doi.org/10.1103/RevModPhys.85.299.

[17] L. Ferrier, E. Wertz, R. Johne, D.D. Solnyshkov, P. Senellart, I. Sagnes, A. Lemaître, G. Malpuech, J. Bloch, Interactions in confined polariton condensates, Phys. Rev. Lett. 106 (2011) 126401, http://dx.doi.org/10.1103/PhysRevLett.106.126401.

[18] N.A. Gippius, I.A. Shelykh, D.D. Solnyshkov, S.S. Gavrilov, Y.G. Rubo, A.V. Kavokin, S.G. Tikhodeev, G. Malpuech, Polarization multistability of cavity polaritons, Phys. Rev. Lett. 98 (2007) 236401, http://dx.doi.org/10.1103/PhysRevLett.98.236401.

[19] T.C.H. Liew, A.V. Kavokin, I.A. Shelykh, Optical circuits based on polariton neurons in semiconductor microcavities, Phys. Rev. Lett. 101 (2008) 016402, http://dx.doi.org/10.1103/PhysRevLett.101.016402.

[20] C. Sturm, D. Tanese, H.S. Nguyen, H. Flayac, E. Galopin, A. Lemaître, I. Sagnes, D. Solnyshkov, A. Amo, G. Malpuech, J. Bloch, All-optical phase modulation in a cavity-polariton Mach–Zehnder interferometer, Nat. Commun. 5 (2014) 3278, http://dx.doi.org/10.1038/ncomms4278.

[21] J. Kasprzak, M. Richard, S. Kundermann, A. Baas, J. Jeambrun, J.M.J. Keeling, F.M. Marchetti, M.H. Szymanska, R. Andre, J.L. Staehli, V. Savona, P.B. Littlewood, B. Deveaud, L.S. Dang, Bose–Einstein condensation of exciton polaritons, Nat. Phys. 443 (2006) 409–414, http://dx.doi.org/10.1038/nature05131.

[22] R. Balili, V. Hartwell, D. Snoke, L. Pfeiffer, K. West, Bose–Einstein condensation of microcavity polaritons in a trap, Science 316 (5827) (2007) 1007–1010, http://dx.doi.org/10.1126/science.1140990.

[23] A. Amo, J. Lefrere, S. Pigeon, C. Adrados, C. Ciuti, I. Carusotto, R. Houdre, E. Giacobino, A. Bramati, Superfluifidy of polaritons in semiconductor microcavities, Nat. Phys. 5 (2009) 805–810, http://dx.doi.org/10.1038/nphys1364.

[24] A. Amo, S. Pigeon, D. Sanvitto, V.G. Sala, R. Hivet, I. Carusotto, F. Pisanello, G. Lemenager, R. Houdre, E. Giacobino, C. Ciuti, A. Bramati, Polariton superfluids reveal quantum hydrodynamic solitons, Science 332 (6034) (2011) 1167–1170, http://dx.doi.org/10.1126/science.1202307.

[25] M. Sich, D.N. Krizhanovskii, M.S. Skolnick, A.V. Gorbach, R. Hartley, D.V. Skryabin, E.A. Cerda-Méndez, K. Biermann, R. Hey, P.V. Santos, Observation of bright polariton solitons in a semiconductor microcavity, Nat. Photonics 6 (1) (2012) 50–55, http://dx.doi.org/10.1038/nphoton.2011.267.

[26] D. Tanese, H. Flayac, D. Solnyshkov, A. Amo, A. Lemaître, E. Galopin, R. Braive, P. Senellart, I. Sagnes, G. Malpuech, J. Bloch, Polariton condensation in solitonic gap states in a one-dimensional periodic potential, Nat. Commun. 4 (2013) 1749, http://dx.doi.org/10.1038/ncomms2760.

[27] P.M. Walker, L. Tinkler, D.V. Skryabin, A. Yulin, B. Royall, I. Farrer, D.A. Ritchie, M.S. Skolnick, D.N. Krizhanovskii, Ultra-low-power hybrid light matter solitons, Nat. Commun. 6 (2015) 8317, http://dx.doi.org/10.1038/ncomms9317.

[28] E.A. Cerda-Méndez, D. Sarkar, D.N. Krizhanovskii, S.S. Gavrilov, K. Biermann, M.S. Skolnick, P.V. Santos, Exciton–polariton gap solitons in two-dimensional lattices, Phys. Rev. Lett. 111 (2013) 146401, http://dx.doi.org/10.1103/PhysRevLett.111.146401.

[29] R. Hivet, H. Flayac, D.D. Solnyshkov, D. Tanese, T. Boulier, D. Andreoli, E. Giacobino, J. Bloch, A. Bramati, G. Malpuech, A. Amo, Half-solitons in a polariton quantum fluid behave like magnetic monopoles, Nat. Phys. 8 (10) (2012) 724–728, http://dx.doi.org/10.1038/nphys2406.

[30] M. Sich, F. Fras, J.K. Chana, M.S. Skolnick, D.N. Krizhanovskii, A.V. Gorbach, R. Hartley, D.V. Skryabin, S.S. Gavrilov, E.A. Cerda-Méndez, K. Biermann, R. Hey, P.V. Santos, Effects of spin-dependent interactions on polarization of bright polariton solitons, Phys. Rev. Lett. 112 (2014) 046403, http://dx.doi.org/10.1103/PhysRevLett.112.046403.

[31] D. Sarkar, S.S. Gavrilov, M. Sich, J.H. Quilter, R.A. Bradley, N.A. Gippius, K. Guda, V.D. Kulakovskii, M.S. Skolnick, D.N. Krizhanovskii, Polarization bistability and resultant spin rings in semiconductor microcavities, Phys. Rev. Lett. 105 (2010) 216402, http://dx.doi.org/10.1103/PhysRevLett.105.216402.

[32] O.A. Egorov, D.V. Skryabin, A.V. Yulin, F. Lederer, Bright cavity polariton solitons, Phys. Rev. Lett. 102 (15) (2009) 153904, http://dx.doi.org/10.1103/PhysRevLett.102.153904.

[33] S. Pigeon, I. Carusotto, C. Ciuti, Hydrodynamic nucleation of vortices and solitons in a resonantly excited polariton superfluid, Phys. Rev. B 83 (2011) 144513, http://dx.doi.org/10.1103/PhysRevB.83.144513.

[34] H. Flayac, D.D. Solnyshkov, G. Malpuech, Oblique half-solitons and their generation in exciton–polariton condensates, Phys. Rev. B 83 (2011) 193305, http://dx.doi.org/10.1103/PhysRevB.83.193305.

[35] A.V. Yulin, D.V. Skryabin, A.V. Gorbach, Dark solitons and vortices in the intrinsic bistability regime in exciton polariton condensates, Phys. Rev. B 92 (2015) 064306, http://dx.doi.org/10.1103/PhysRevB.92.064306.

[36] N.S. Voronova, Y.E. Lozovik, Excitons in cores of exciton–polariton vortices, Phys. Rev. B 86 (2012) 195305, http://dx.doi.org/10.1103/PhysRevB.86.195305.

[37] Y.S. Kivshar, D.E. Pelinovsky, Self-focusing and transverse instabilities of solitary waves, Phys. Rep. 331 (4) (2000) 117–195, http://dx.doi.org/10.1016/S0370-1573(99)00106-4.

[38] O.A. Egorov, A.V. Gorbach, F. Lederer, D.V. Skryabin, Two-dimensional localization of exciton polaritons in microcavities, Phys. Rev. Lett. 105 (7) (2010) 073903, http://dx.doi.org/10.1103/PhysRevLett.105.073903.

[39] O.A. Egorov, D.V. Skryabin, F. Lederer, Parametric polariton solitons in coherently pumped semiconductor microcavities, Phys. Rev. B 84 (2011) 165305, http://dx.doi.org/10.1103/PhysRevB.84.165305.

[40] O.A. Egorov, D.V. Skryabin, F. Lederer, Polariton solitons due to saturation of the exciton–photon coupling, Phys. Rev. B 82 (2010) 165326, http://dx.doi.org/10.1103/PhysRevB.82.165326.

[41] I.V. Barashenkov, E.V. Zemlyanaya, Existence threshold for the AC-driven damped nonlinear Schrödinger solitons, Physica D 132 (3) (1999) 363–372, http://dx.doi.org/10.1016/S0167-2789(99)00055-X.

[42] D.V. Skryabin, Energy of the soliton internal modes and broken symmetries in nonlinear optics, J. Opt. Soc. Am. B 19 (3) (2002) 529–536, http://dx.doi.org/10.1364/JOSAB.19.000529.

[43] G. Slavcheva, A.V. Gorbach, A. Pimenov, A.G. Vladimirov, D.V. Skryabin, Multi-stability and polariton solitons in microcavity wires, Opt. Lett. 40 (8) (2015) 1787–1790, http://dx.doi.org/10.1364/OL.40.001787.

[44] A.V. Yulin, O.A. Egorov, F. Lederer, D.V. Skryabin, Dark polariton solitons in semiconductor microcavities, Phys. Rev. A 78 (2008) 061801, http://dx.doi.org/10.1103/PhysRevA.78.061801.

[45] A. Werner, O.A. Egorov, F. Lederer, Spin dynamics of dark polariton solitons, Phys. Rev. B 85 (2012) 115315, http://dx.doi.org/10.1103/PhysRevB.85.115315.

[46] G. Grosso, G. Nardin, F. Morier-Genoud, Y. Léger, B. Deveaud-Plédran, Soliton instabilities and vortex street formation in a polariton quantum fluid, Phys. Rev. Lett. 107 (2011) 245301, http://dx.doi.org/10.1103/PhysRevLett.107.245301.

[47] P. Cilibrizzi, H. Ohadi, T. Ostatnicky, A. Askitopoulos, W. Langbein, P. Lagoudakis, Linear wave dynamics explains observations attributed to dark solitons in a polariton quantum fluid, Phys. Rev. Lett. 113 (2014) 103901, http://dx.doi.org/10.1103/PhysRevLett.113.103901.

[48] A. Amo, J. Bloch, A. Bramati, I. Carusotto, C. Ciuti, B. Deveaud, E. Giacobino, G. Grosso, A. Kamchatnov, G. Malpuech, N. Pavloff, S. Pigeon, D. Sanvitto, D.D. Solnyshkov, Comment on "Linear wave dynamics explains observations attributed to dark solitons in a polariton quantum fluid", Phys. Rev. Lett. 115 (2015) 089401, http://dx.doi.org/10.1103/PhysRevLett.115.089401.

[49] A. Kavokin, G. Malpuech, M. Glazov, Optical spin Hall effect, Phys. Rev. Lett. 95 (2005) 136601, http://dx.doi.org/10.1103/PhysRevLett.95.136601.

[50] H. Flayac, D.D. Solnyshkov, I.A. Shelykh, G. Malpuech, Transmutation of Skyrmions to half-solitons driven by the nonlinear optical spin Hall effect, Phys. Rev. Lett. 110 (2013) 016404, http://dx.doi.org/10.1103/PhysRevLett.110.016404.

[51] Y.V. Kartashov, B.A. Malomed, L. Torner, Solitons in nonlinear lattices, Rev. Mod. Phys. 83 (2011) 247–305, http://dx.doi.org/10.1103/RevModPhys.83.247.

[52] J.K. Chana, M. Sich, F. Fras, A.V. Gorbach, D.V. Skryabin, E. Cancellieri, E.A. Cerda-Méndez, K. Biermann, R. Hey, P.V. Santos, M.S. Skolnick, D.N. Krizhanovskii, Spatial patterns of dissipative polariton solitons in semiconductor microcavities, Phys. Rev. Lett. 115 (2015) 256401, http://dx.doi.org/10.1103/PhysRevLett.115.256401.

[53] E. Cancellieri, J.K. Chana, M. Sich, D.N. Krizhanovskii, M.S. Skolnick, D.M. Whittaker, Logic gates with bright dissipative polariton solitons in Bragg cavity systems, Phys. Rev. B 92 (2015) 174528, http://dx.doi.org/10.1103/PhysRevB.92.174528.

[54] J.P. Karr, A. Baas, R. Houdré, E. Giacobino, Squeezing in semiconductor microcavities in the strong-coupling regime, Phys. Rev. A 69 (2004) 031802, http://dx.doi.org/10.1103/PhysRevA.69.031802.

[55] T. Boulier, M. Bamba, A. Amo, C. Adrados, A. Lemaitre, E. Galopin, I. Sagnes, J. Bloch, C. Ciuti, E. Giacobino, A. Bramati, Polariton-generated intensity squeezing in semiconductor micropillars, Nat. Commun. 5 (2014) 3260, http://dx.doi.org/10.1038/ncomms4260.

[56] A.V. Nalitov, D.D. Solnyshkov, G. Malpuech, Polariton $\mathbb{Z}$ topological insulator, Phys. Rev. Lett. 114 (2015) 116401, http://dx.doi.org/10.1103/PhysRevLett.114.116401.

[57] T. Karzig, C.-E. Bardyn, N.H. Lindner, G. Refael, Topological polaritons, Phys. Rev. X 5 (2015) 031001, http://dx.doi.org/10.1103/PhysRevX.5.031001.

[58] Y. Lumer, Y. Plotnik, M.C. Rechtsman, M. Segev, Self-localized states in photonic topological insulators, Phys. Rev. Lett. 111 (2013) 243905, http://dx.doi.org/10.1103/PhysRevLett.111.243905.